OCCURRENCE AND ORIGIN OF LUNAR PITS: OBSERVATIONS FROM A NEW CATALOG. R. V. Wagner and M. S. Robinson, School of Earth and Space Exploration, Arizona State University, Tempe, AZ 85287-3603 (rvwagner@asu.edu).

Introduction: Lunar pits are small collapse features (10s to 100s of meter scale) characterized by vertical walls **[1]**, as distinct from the kilometer-scale conical pit craters that are often found in chains along graben (e.g. Rima Hyginus). Lunar pits provide cross-section exposures up to 100 m thick through their host terrains, and perhaps even enable access to subsurface void spaces **[1,2,3]** that could provide shelter for future explorers. To date, we have identified ~281 pits in melt deposits of impact craters, 15 pits in mare basalts, and 5 pits in non-impact-melt highland terrain. We are now releasing a catalog documenting morphologic parameters along with a brief description of each pit.

Using the observations presented in this catalog, along with previous work on the morphologies of mare pits **[4]**, we evaluated hypotheses for the formation of lunar pits. While similar features on Mars sometimes show evidence of access to extant lava tubes **[5,6,7]**, none of the lunar examples exhibit landforms definitively related to formation by collapse into lava tubes.

Origins of Voids: The nature of the void spaces into which lunar pits collapsed is an open question. Collapse into a lava tube is a common suggestion for mare pit origin, and detections of an intact lava tube near the Marius Hills pit have been reported **[3,8]**, but these interpretations are not conclusive. Alternate mechanisms, such as stoping of tectonically- or magmatically-formed voids **[9]**, could produce the observed pit morphologies without a tube system.

The most commonly cited evidence from terrestrial remote sensing observations for identifying pits opening into lava tubes is their occurrence as a sinuous chain or within a sinuous topographic feature; this formation pattern also occurs on Mars **[6,7]**. On the Moon, however, no pits occur in distinctly sinuous chains, and while a few impact melt pits occur within linear or arcuate depressions, of the mare pits, only the Marius Hills pit lies within a sinuous depression. The strongest indicator of a potential lava tube related to a pit is linear collapse feature crossing a wrinkle ridge, aligned with the West Marius Hills pit (45 km from Marius Hills pit; **Fig. 1A**). This evidence suggests that the West Marius Hills (and perhaps Marius Hills) pits may have collapsed into lava tubes. However, no other mare or highland pits have similar indicators of a relation to a lava tube. In two cases (Ingenii, Schlüter), pits occur within one crater radius of >600m diameter craters (**Fig. 1B,C**), which could reasonably be expected to fully collapse a near-surface lava tube **[10]**, rather than leaving an intact tube with a single hole in the roof.

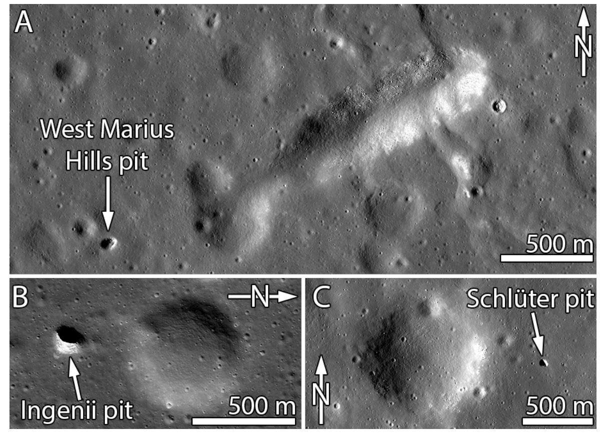

Figure 1: *A)* West Marius Hills pit and possible collapsed lava tube. *B,C)* Large impact craters near pits, without similar large-scale tube collapses.

While several mare pits occur within a few kilometers of tectonic features (of particular note: Southwest Fecunditatis, in a region of extensional stress with several nearby graben), this number is not higher than would be expected for a random distribution of pits.

Impact melt pit origins. Impact melt pits that lie within depressions are mostly in linear or (especially in Copernicus crater) arcuate depressions similar to the shape of surface fractures in melt ponds. Of the 12 pit clusters with >2 pits each, half are linearly aligned, and none could be described as "sinuous". These occurrences suggest that many impact melt pits originated with fracturing of the melt pond crust as the melt cooled and as the terrain isostatically rebounded from the impact event, even where no surface fractures are visible.

Another class of impact melt pit seem unrelated to fracturing. These pits occur on positive relief features and are especially common in the King crater melt pond. In particular, the King 1 pair of pits (on the flank of a small dome; **Fig. 2**) are separated by a natural arch, which would probably not have survived extensional deformation. Slewed images show an overhang extending at least few meters under the dome, and the arch itself is part of the dome's original surface, suggesting that the dome was originally hollow.

Pit Catalog: For each pit, we have recorded the location, dimensions, and various feature descriptors (such as whether the pit is within a positive or negative relief feature, or has a path to the floor uninterrupted by a vertical wall), as well as a detailed description of the pit and environs. Where possible, depths are calculated from shadow measurements on three minimally-slewed images. Each pit is named based on the host feature's name, usually followed by a number roughly corresponding to order of discovery and a letter if the pit is part of a multi-pit cluster (e.g. "King 1a" and "King 1b"; see **Fig. 2**). A draft version of a catalog page for one pit is shown in **Fig. 2**.

Latitude and longitude coordinates were computed from an average of multiple images and so should be more accurate than the ~30 m uncertainty of an arbitrary NAC image **[11]**. However, we also report the line/sample location of the center of each pit in one LROC NAC frame to ensure unambiguous identification of each pit regardless of any future updates to the LROC ephemeris or changes to the lunar reference frame.

This catalog also includes some notable "fracture-associated" pits (pits physically connected to the fractures commonly found on impact melt surfaces), which, while not falling within the definition of "pit" used in **[1]**, may be useful from an engineering or habitability perspective. Fracture-associated pits were excluded in **[1]** due to sheer abundance and the difficulty in arbitrarily defining a cut-off between "fracture" and "pit", making it impractical to provide a full accounting of them.

Release Plan. The full catalog will be released in March 2021 in three formats: A Comma-Separated Values (CSV) file and matching ESRI shapefile in the LROC PDS archive, a set of online detail pages with images of each pit, and a PDF version of the same

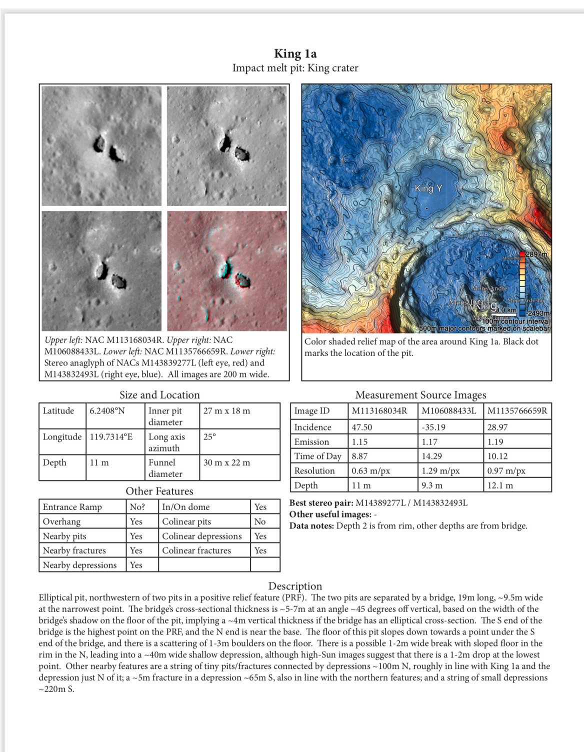

King 1a
Impact melt pit: King crater

Upper left: NAC M113168034R. *Upper right:* NAC M106088433L. *Lower left:* NAC M1135766659R. *Lower right:* Stereo anaglyph of NACs M143839277L (left eye, red) and M143832493L (right eye, blue). All images are 200 m wide.

Color shaded relief map of the area around King 1a. Black dot marks the location of the pit.

Size and Location

Latitude	6.2408°N	Inner pit diameter	27 m x 18 m
Longitude	119.7314°E	Long axis azimuth	25°
Depth	11 m	Funnel diameter	30 m x 22 m

Measurement Source Images

Image ID	M113168034R	M106088433L	M1135766659R
Incidence	47.50	-35.19	28.97
Emission	1.15	1.17	1.19
Time of Day	8.87	14.29	10.12
Resolution	0.63 m/px	1.29 m/px	0.97 m/px
Depth	11 m	9.3 m	12.1 m

Other Features

Entrance Ramp	No?	In/On dome	Yes
Overhang	Yes	Colinear pits	No
Nearby pits	Yes	Colinear depressions	Yes
Nearby fractures	Yes	Colinear fractures	Yes
Nearby depressions	Yes		

Best stereo pair: M14389277L / M143832493L
Other useful images: -
Data notes: Depth 2 is from rim, other depths are from bridge.

Description

Elliptical pit, northwestern of two pits in a positive relief feature (PRF). The two pits are separated by a bridge, 19m long, ~9.5m wide at the narrowest point. The bridge's cross-sectional thickness is ~5-7m at an angle ~45 degrees off vertical, based on the width of the bridge's shadow on the floor of the pit, implying a ~4m vertical thickness if the bridge has an elliptical cross-section. The S end of the bridge is the highest point on the PRF, and the N end is near the base. The floor of this pit slopes down towards a point under the S end of the bridge, and there is a scattering of 1-3m boulders on the floor. There is a possible 1-2m wide break with sloped floor in the rim in the N, leading into a ~40m wide shallow depression, although high-Sun images suggest that there is a 1-2m drop at the lowest point. Other nearby features are a string of tiny pits/fractures connected by depressions ~100m N, roughly in line with King 1a and the depression just N of it; a ~5m fracture in a depression ~65m S, also in line with the northern features; and a string of small depressions ~220m S.

Figure 3: Draft page from the pit catalog PDF.

(**Fig. 2**). The latter two versions will be similar to the Permanently Shadowed Region Atlas previously published by the LROC team **[12]**.

Statistical notes. As an example of analyses this catalog enables, we present a few statistics. Pits mentioned in this section are shown in **Fig. 3**.

Impact melt pit depth/diameter ratios range from 0.08 (Crookes 1) to 2.8 (King 8b) or >3.5 (Copernicus 7) (mean = 0.67), while mare and highland pits range from 0.17 (Mare Insularum) to 2.5 (Southwest Fecunditatis) (mean = 0.64).

Potential pits with diameters < 5 m were excluded from the catalog due to usually being too small to confirm as pits with LROC NAC images. With that caveat, the median impact melt pit diameter is 15 m (range 5-385 m), the median mare pit is 100 m (17-175 m), and the median highland pit is 45 m (16-65 m).

Conclusion: Each mare and highland pit will need to be evaluated on its own merits to determine likely origin processes. The West Marius Hills pit is consistent with an origin involving collapse into an extant lava tube, but we have not observed strong evidence that other mare pits open into a lava tube. Impact melt pit void spaces are probably often created by stresses from deformation as the melt cools and the local terrain rebounds, though much like mare pits, there may be several origins for the underlying void spaces.

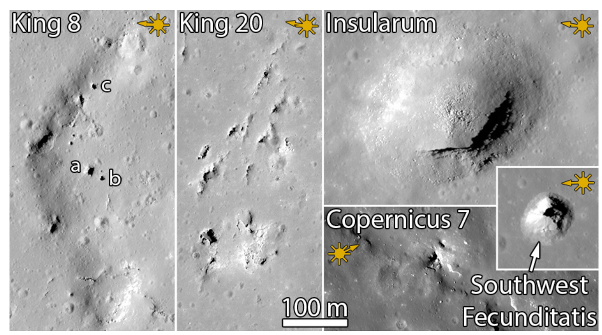

Figure 3: Assorted pits, at identical scales.

References: **[1]** Wagner and Robinson (2014), *Icarus*, *237C*, 52–60. doi: 10.1016/j.icarus.2014.04.002. **[2]** Haruyama et al. (2009), *Geophys. Res. Lett.*, *36*, L21206, doi: 10.1029/2009GL040635. **[3]** Chappaz et al. (2017), *Geophys. Res. Lett.*, *44*, 1, 0105-112. doi: 10.1002/2016GL071588 **[4]** Wagner and Robinson (2019), *50th LPSC,* #2138 **[5]** Cushing et al. (2015), *JGR*, *120*, 1023-1043. doi: 10.1002/2014JE004735 **[6]** Cushing (2015), Mars Global Cave Candidate Catalog PDS4 Archive Bundle. doi: 10.17189/1519222 **[7]** Sauro et al. (2020) *Earth Sci. Rev.* doi: 10.1016/j.earscirev.2020.103288 **[8]** Kaku et al. (2017) *Geophys. Res. Lett.*, *44*, doi: 10.1002/2017GL074998 **[9]** Okubo and Martel (1998), *J. Volc. And Geotherm. Res.*, 86, 1-18. **[10]** Melosh (1989) Impact Cratering. **[10]** Wagner et al. (2017), *Icarus*, 283, 92-103. doi: 10.1016/j.icarus.2016.05.011 **[11]** Cisneros et al. (2017), *48th LPSC,* #2469.